



ARTICLE

The M1/M4 preferring muscarinic agonist xanomeline modulates functional connectivity and NMDAR antagonist-induced changes in the mouse brain

Caterina Montani^{1,5}, Carola Canella¹, Adam J. Schwarz^{2,4}, Jennifer Li³, Gary Gilmour³, Alberto Galbusera¹, Keith Wafford³, Daniel Gutierrez-Barragan¹, Andrew McCarthy³, David Shaw², Karen Knitowski², David McKinzie^{2,5}, Alessandro Gozzi¹ and Christian Felder^{2,6}

Cholinergic drugs acting at M1/M4 muscarinic receptors hold promise for the treatment of symptoms associated with brain disorders characterized by cognitive impairment, mood disturbances, or psychosis, such as Alzheimer's disease or schizophrenia. However, the brain-wide functional substrates engaged by muscarinic agonists remain poorly understood. Here we used a combination of pharmacological fMRI (phMRI), resting-state fMRI (rsfMRI), and resting-state quantitative EEG (qEEG) to investigate the effects of a behaviorally active dose of the M1/M4-preferring muscarinic agonist xanomeline on brain functional activity in the rodent brain. We investigated both the effects of xanomeline per se and its modulatory effects on signals elicited by the NMDA-receptor antagonists phencyclidine (PCP) and ketamine. We found that xanomeline induces robust and widespread BOLD signal phMRI amplitude increases and decreased high-frequency qEEG spectral activity. rsfMRI mapping in the mouse revealed that xanomeline robustly decreased neocortical and striatal connectivity but induces focal increases in functional connectivity within the nucleus accumbens and basal forebrain. Notably, xanomeline pre-administration robustly attenuated both the cortico-limbic phMRI response and the fronto-hippocampal hyper-connectivity induced by PCP, enhanced PCP-modulated functional connectivity locally within the nucleus accumbens and basal forebrain, and reversed the gamma and high-frequency qEEG power increases induced by ketamine. Collectively, these results show that xanomeline robustly induces both cholinergic-like neocortical activation and desynchronization of functional networks in the mammalian brain. These effects could serve as a translatable biomarker for future clinical investigations of muscarinic agents, and bear mechanistic relevance for the putative therapeutic effect of these class of compounds in brain disorders.

Neuropsychopharmacology (2021) 46:1194–1206; <https://doi.org/10.1038/s41386-020-00916-0>

INTRODUCTION

Xanomeline is a muscarinic-receptor agonist derived from a natural muscarinic agonist, arecoline, an active ingredient of betel nut, chewing of which is common in Asian and Pacific cultures. Xanomeline exhibits partial selectivity for M1 and M4 muscarinic receptors, and lower, yet non-negligible, affinity for M2, M3, and M5 receptor subtypes [1–5]. The cholinergic system has been described as a widely distributed neuromodulatory system [6] whose sources include local interneurons that are present in multiple brain regions, and cholinergic projection neurons that produce and release acetylcholine from two distinct clusters: basal forebrain nuclei which innervate cortical, hippocampal, and thalamic areas; and the brainstem nuclei which innervate midbrain, hindbrain, thalamic, and cerebellar areas [7].

An increasing body of evidence has highlighted a potential beneficial effect of cholinergic stimulation on brain disorders characterized by cognitive dysfunction or psychosis, including neurodegenerative conditions such as Alzheimer's disease (AD) or neuropsychiatric diseases such as schizophrenia [8–10]. These properties have prompted clinical investigations into the use of this drug to improve cognitive function and behavioral disturbance in AD patients, with encouraging results, but dose-limiting peripheral cholinergic side effects [11–16]. Interestingly, a parallel set of clinical observations have linked recreational use of betel nut with fewer positive and negative symptoms in schizophrenia [17], a finding that has been linked to the observation of decreased M1/M4 mAChR density in the brains of schizophrenia patients (reviewed by [18]). These anecdotal findings have been corroborated by subsequent research demonstrating putative

¹Functional Neuroimaging Laboratory, Istituto Italiano di Tecnologia, Center for Neuroscience and Cognitive Systems @ UniTn, 38068 Rovereto, Italy; ²Eli Lilly and Company, Indianapolis, IN 46285, USA and ³Eli Lilly and Company, Windlesham, UK

Correspondence: Alessandro Gozzi (alessandro.gozzi@iit.it)

⁴Present address: Takeda Pharmaceuticals Ltd., Cambridge, MA 01240, USA

⁵Present address: Indiana University School of Medicine, Indianapolis, IN 46202, USA

⁶Present address: Karuna Therapeutics, Boston, MA 02110, USA

These authors contributed equally: Caterina Montani, Carola Canella, Adam J. Schwarz.

These authors jointly supervised this work: Adam J. Schwarz, Alessandro Gozzi, Christian Felder.

Received: 7 May 2020 Revised: 2 October 2020 Accepted: 10 November 2020

Published online: 20 December 2020

antipsychotic properties of xanomeline in preclinical and clinical studies. Specifically, treatment with xanomeline has been reported to inhibit the behavioral and motor effects of amphetamine and apomorphine in monkeys [2] and to produce behavioral responses in rodents similar to those seen after treatment with traditional antipsychotics [1, 19, 20]. In keeping with this, recent clinical studies have demonstrated that monotherapy with xanomeline can improve positive and negative symptoms as well as cognitive function in human subjects with schizophrenia [21].

While previous studies have addressed neurochemical and behavioral consequences of muscarinic modulation [3, 22, 23] the macroscopic brain circuits and functional substrates engaged by M1/M4 agonism, and xanomeline in particular, remain poorly investigated. One previous study reported that xanomeline dose-dependently reversed the ketamine-evoked pharmacological fMRI (phMRI) signal increases in the rat brain, demonstrating a modulating effect of muscarinic agonism on an aberrant glutamatergic state considered of mechanistic relevance to schizophrenia [24]. Since ketamine-challenge phMRI has been successfully translated into healthy humans and modulated by both clinically approved drugs and novel glutamatergic agents [25–29], this observation indicates a potential translational biomarker opportunity. Complementary to this approach, a deeper understanding of the central effects of xanomeline could be obtained by profiling its effect on interregional fMRI synchronization, or “functional connectivity”, in distributed brain circuits via resting-state fMRI (rsfMRI) [30, 31]. In addition, oxygen (O₂) amperometry provides a complementary method to measure the local hemodynamic response in conscious mobile animals [32, 33], and quantitative electro-encephalography (qEEG) provides a means of monitoring the power-frequency profile of the brain’s electrical rhythms more directly, unfiltered by the hemodynamic response underlying the fMRI signals [34, 35]. Given the established role of cholinergic systems in arousal and neocortical excitation, cholinergic modulation could conceivably affect large-scale cortical coupling and electrical activity of the brain, resulting in rsfMRI- and qEEG-detectable effects. A characterization of such effects could provide a robust, multimodal description of the pharmacological properties of this class of compounds of high mechanistic and translational relevance.

Here, we used fMRI, O₂ amperometry, and qEEG to characterize the brain-wide functional substrates modulated by the M1/M4-preferring muscarinic agonist xanomeline in mice and rats. To mechanistically relate xanomeline-induced functional changes to the putative antipsychotic properties of this compound, we also assessed the drug’s ability to modulate or prevent brain signals elicited by the noncompetitive NMDA-receptor (NMDAR) antagonists phencyclidine (PCP) and ketamine, compounds that produce robust schizophrenia-like syndromes and stereotypical fMRI, O₂ amperometric and qEEG responses in rodents [36–42]. Together, these multimodal experiments provide a comprehensive picture of the effects of xanomeline on brain-wide functional activity, desynchronization of neocortical networks, and its modulatory effects on specific NMDAR antagonist-induced network aberrancies.

MATERIALS AND METHODS

A complete description of the experimental procedures can be found in the “Extended Methods” in the Supplementary Information section.

Ethical statement

fMRI studies were conducted in accordance with the Italian law (DL 116, 1992 Ministero della Sanità, Roma), the recommendations in the Guide for the Care and Use of Laboratory Animals of the National Institutes of Health and consented to by the animal care committee of the Istituto Italiano di Tecnologia. O₂

amperometry and EEG experiments were conducted in accordance with the Animals (Scientific Procedures) Act 1986 (UK) following approval from the local Animal Welfare and Ethics Review Body.

Conditioned avoidance responding (CAR)

Conditioned avoidance responding (CAR) was conducted in standard shuttle boxes as previously described [43]. Mice were first trained to avoid shock at criterion-level performance ($\geq 90\%$ avoidance responding) and then saline and xanomeline tartrate (1, 3, 10, and 30 mg/kg) were administered via intraperitoneal (i.p.) injection 30 min prior to behavioral testing.

Spontaneous and PCP-induced locomotor activity (LMA)

Locomotor activity (LMA) was conducted in an open field apparatus which recorded horizontal photobeam breaks. On the test day, mice received a dose of saline or xanomeline tartrate (1, 3, 10, or 30 mg/kg s.c.) and were placed into the open field for a 30-min period to measure the effects of xanomeline alone upon LMA. Then, 5 mg/kg PCP HCl was administered (s.c.) to all mice, which were then returned to the open field for the 60-min PCP-induced activity phase. Total horizontal activity counts were analyzed.

fMRI

The animal preparation protocol for fMRI was described in detail [44–46]. fMRI data were acquired with a 7.0 Tesla MRI scanner (Bruker Biospin, Milan) using intrapulmonary halothane anesthesia (0.75%). Two consecutive 30-min BOLD fMRI time series were acquired; during the first, either vehicle (saline) or xanomeline (30 mg/kg) was administered (s.c.) after 10 min; during the second, either PCP (1 mg/kg) or vehicle (saline) was administered intravenously (i.v.) after 10 min.

Plasma xanomeline/PCP quantification

Plasma quantification was performed as previously described [47]. Blood samples were taken from the cannulated femoral artery at the end of fMRI experiments. Plasma was obtained and stored at $-20\text{ }^{\circ}\text{C}$ until quantification, which was performed by Eli Lilly Inc., Indianapolis.

In vivo O₂ amperometry

Changes in extracellular tissue [O₂] were measured using constant potential amperometry [32]. Animals were cabled for 30 min pre-injection to establish a stable baseline and then treated with either vehicle or the relevant dose of xanomeline (1, 3, or 10 mg/kg i.p.) and oxygen signals recorded for 90 min.

EEG

Chronic measurement of EEG and electromyogram was conducted as previously described by [48, 49]. Baseline wake, NREM sleep, and REM sleep were calculated for 24 h prior to dosing. Drug treatments occurred 4.5–5 h after lights. Xanomeline was dosed (s.c.) at 1, 3, and 10 mg/kg and ketamine (s.c.) at 10 mg/kg 30 min later. The effects of the compounds were evaluated over the first 7-h light phase following treatment.

RESULTS

Dose selection

To ensure behavioral relevance of the effects mapped with fMRI, we selected the xanomeline dose based on two independent behavioral assays performed in C57Bl/6NTac and naive, ICR outbred mice. In the first of these assays (Fig. S1A), we measured the ability of xanomeline administration to disrupt conditioned avoidance response. In the second assay (Fig. S1B), we measured the effect of xanomeline administration on both spontaneous and PCP-induced LMA. In both assays, a dose of 30 mg/kg xanomeline

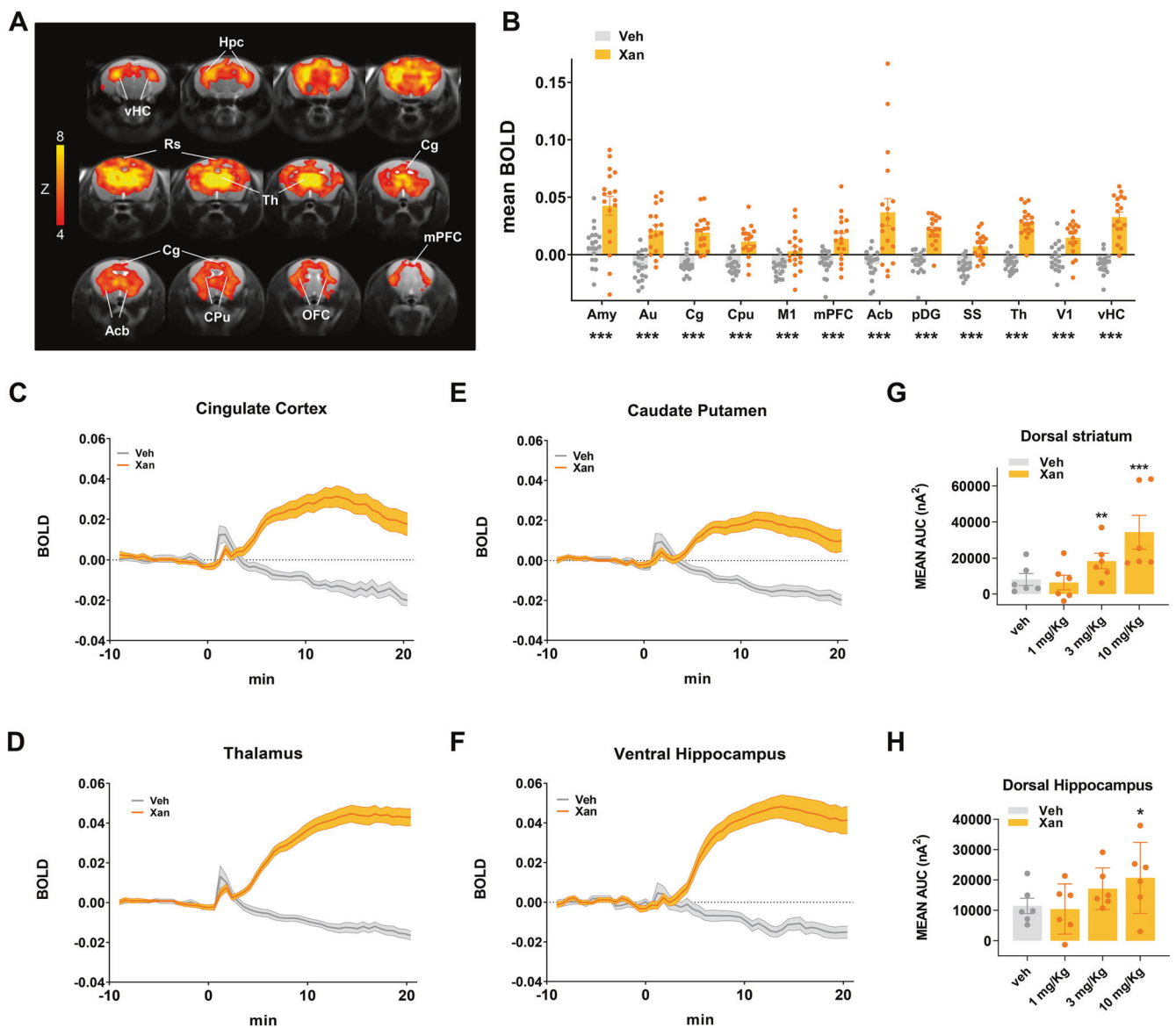


Fig. 1 Xanomeline increases functional brain activity as measured with BOLD fMRI and O₂ amperometry in the mouse. **A** Maps of BOLD fMRI response elicited by a xanomeline challenge (30 mg/kg s.c.) with respect to the vehicle-treated control group. Orange/yellow indicate increases in BOLD signal ($Z > 4$, $p < 0.05$, cluster corrected). **B** BOLD response to xanomeline in representative ROIs. The effect was plotted as mean BOLD \pm SEM. (t -test, $*p < 0.05$, $**p < 0.01$, $***p < 0.001$, FDR corrected). Time course of BOLD signal in cingulate cortex (**C**), thalamus (**D**) caudate putamen (**E**), and ventral hippocampus (**F**), respectively. Xanomeline was injected at time 0. Vehicle $n = 19$, xanomeline $n = 18$. O₂ amperometry changes showing dose-dependent increases measured by probes positioned in the dorsal striatum (**G**) and dorsal hippocampus (**H**). Effects are plotted as mean amperometric current \pm SEM. (Fishers LSD, $*p < 0.05$, $**p < 0.01$, $***p < 0.001$, versus vehicle group). Amy amygdala, Au auditory cortex, Cg cingulate cortex, Cpu caudate putamen, M1 primary motor cortex, mPFC medial prefrontal cortex, Acb accumbens, pDG posterior dentate gyrus, SS somatosensory cortex, Th thalamus, V1 primary visual cortex, vHC ventral hippocampus, VTA ventral tegmental area, Hpc hippocampus, Rs retrosplenial cortex, OFC orbitofrontal cortex.

(i.p. or s.c., respectively) produced maximal efficacy, as demonstrated by complete inhibition of avoidance responses ($p < 0.0125$, Bonferroni-corrected) and reversal of PCP-induced LMA ($F_{4,35} = 17.17$, $p < 0.0001$; Dunnett test, $p < 0.05$ vs. vehicle). While escape failures during conditioned avoidance testing were not significantly induced by administration of xanomeline tartrate ($F_{4,36} = 1.00$, $p > 0.42$), spontaneous LMA was reduced ($F_{4, 35} = 21.34$, $p < 0.0001$, Dunnett test, $p < 0.05$ vs. vehicle). Based on these results, a dose of 30 mg/kg was selected for testing in imaging studies.

Xanomeline produces robust brain-wide functional activation
Acute administration of xanomeline in C57Bl6/J mice produced robust BOLD pHMRI responses in widespread brain regions,

including retrosplenial, cingulate, medial prefrontal and orbitofrontal cortices, the thalamus, dorsal hippocampal areas, basal ganglia and nucleus accumbens (Fig. 1A–D, volume of interest location, Fig. S2). The temporal BOLD profile following xanomeline administration revealed a gradual increase in BOLD signal, reaching a maximum in cortical regions ~15 min after the injection. Importantly, the peripheral blood pressure recordings (Fig. S3) showed that xanomeline-induced increases remained within autoregulation range under halothane anesthesia for almost all of the time window imaged [50], arguing against a nonspecific peripheral hemodynamic contribution to the observed functional changes. To corroborate these findings in non-anesthetized animals, we measured the oxygen

amperometric response produced by xanomeline in the dorsal striatum and dorsal hippocampus of freely behaving C57BL/6NTac mice (Fig. 1G, H). Dose-dependent increases in tissue O_2 levels were observed in both regions (Region \times Dose interaction: $F_{3, 15} = 4.86$, $p = 0.0147$). In dorsal striatum, both the 3 and 10 mg/kg doses of xanomeline significantly increased tissue O_2 (Fishers LSD: $p = 0.0143$ and $p > 0.0001$, respectively) relative to vehicle, while the 10 mg/kg dose was significant for the dorsal hippocampus (Fishers LSD: $p = 0.0253$). Plasma drug level measurements at the end of the fMRI experiments are reported in Fig. S4. These measurements confirmed successful compound exposure in all animals analyzed in this study, and did not reveal statistical significant differences across cohorts ($p > 0.22$, all groups). We also report in Table S1 the potency of xanomeline at different receptor subtypes for reference (modified from [4]).

Xanomeline decreases local and long-range brain functional connectivity

To map local and long-range functional connectivity changes produced by xanomeline in the mouse brain, we used recently developed summary metrics described in detail elsewhere [51]. Xanomeline administration revealed a robust and widespread reduction in both local and long-range connectivity ($t > 3$, $p < 0.05$, cluster corrected, Fig. 2A). The effect was especially prominent in cortical regions such as the anterior cingulate, primary motor, auditory, somatosensory, and retrosplenial cortices. Interestingly, foci of increased local (but not long range) connectivity were observed in basal forebrain areas and in the nucleus accumbens (Fig. 2A). Quantification in areas of interest (Fig. 2B, C) corroborated these findings.

Xanomeline reduces connectivity of interhemispheric and antero-posterior networks

To better identify the specific networks underlying local and long-range connectivity deficits, we used seed-based mapping to probe xanomeline modulatory effects in known mouse brain rsfMRI connectivity networks (Fig. 2D–F). These analyses revealed the presence of reduced interhemispheric cortico-cortical connectivity in several motor sensory cortical districts (i.e., visual, motor, auditory) and in the dorsal hippocampus. Similarly, functional probing of the anterior cingulate cortex revealed reduced antero-posterior functional connectivity across areas of the mouse default mode network (DMN). Interestingly, the nucleus accumbens appeared to be locally hyper-connected, consistent with the increase in the local connectivity parameter described above. A quantification of these effects in the region of interests corroborated these effects (Fig. 2E, F).

Xanomeline increases wakefulness and decreases EEG power

To complement the fMRI and amperometric O_2 measures in the mouse and learn more about the neural effects of the drug, xanomeline was also dosed to Wistar rats implanted with EEG electrodes to measure sleep/wake and EEG spectral activity parameters. Drug was administered subcutaneously 5 h after lights on. At 1, 3, and 10 mg/kg xanomeline elicited dose-dependent, robust increases in wakefulness with 37 ± 13 ($p = 0.038$), 110 ± 13 ($p < 0.001$), and 225 ± 13 ($p < 0.001$) minutes of additional wake over the first 7 h relative to baseline (Fig. 3A). At 10 mg/kg the increased wake extended into the subsequent dark period, and no rebound sleep occurred as a consequence of the extended wakefulness. Spectral activity occurring during this induced waking was significantly affected with reduction in the alpha and beta range ($p < 0.001$), as well as reduction in the high-frequency range (above 80 Hz) ($p < 0.01$ at 3 mg/kg and $p < 0.001$ at 10 mg/kg) (Fig. 3B, C). Any periods of sleep that were identified in the 7 h post dosing were significantly depleted in delta power (data not shown).

Xanomeline attenuates the locomotor and BOLD fMRI response to the NMDAR antagonist PCP

In a subsequent set of mouse studies we assessed the modulatory effect of xanomeline on the functional response elicited by subanesthetic dosing of PCP, an NMDAR antagonist with psychotomimetic properties. Acute administration of PCP (1 mg/kg, $n = 10$) induced robust BOLD fMRI activation of a set of cortico-limbo-thalamic regions previously reported to be activated by NMDAR antagonists in rodents (Fig. 4A) [30, 41]. The temporal profile of PCP-induced activation (Fig. 4B) was similar across activated brain structures with a rapid signal increase followed by a sustained activation lasting throughout the imaging window.

As reported above, preliminary behavioral assessments revealed that the dose of xanomeline employed in fMRI studies (30 mg/kg) was able to robustly inhibit the locomotor response produced by acute administration of PCP (Fig. S1B), an effect that however at the highest doses could be partly reflect a reduction in baseline LMA produced by xanomeline treatment per se. In our subsequent pHMRI study we found that pretreatment with xanomeline robustly attenuated the BOLD response to PCP in across much of the activated areas (anterior cingulate cortex, retrosplenial cortex, primary motor cortex, ventral hippocampus, primary visual cortex, $Z > 2$, cluster corrected) (Fig. 4A). When quantified in regions of interest the effect of xanomeline reached statistical significance in most of the examined regions (Fig. 4C). Although the response reduction appeared to be rather widespread, complete response blockade was apparent only in selected brain areas, such as cingulate cortex, striatum, ventral hippocampus, and sensorimotor regions.

Xanomeline decreases ketamine-induced changes in gamma and high-frequency EEG activity

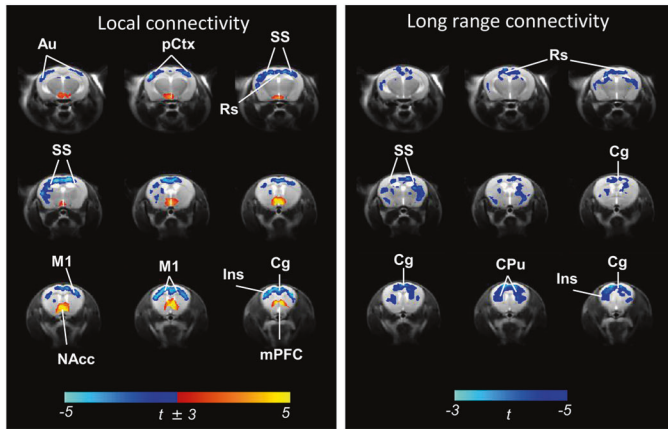
NMDAR antagonists such as ketamine and PCP have been shown to boost high-frequency EEG oscillations with increases in the gamma and high-frequency oscillation (HFO) range [52] and decreases in the beta frequency range [53]. To probe whether xanomeline pretreatment could prevent this EEG response, we pretreated Wistar rats with 10 mg/kg xanomeline s.c. followed 30 min later by a dose of 10 mg/kg (S+)ketamine s.c. at CT-5. Both drugs promoted wakefulness and this was unchanged in the dual-dosed rats (data not shown). The decrease in alpha/beta power was not significantly different with xanomeline, or xanomeline and ketamine, however the ketamine-induced increase in gamma power and particularly the HFO (130–160 Hz) were reduced by pretreatment with xanomeline (Fig. 4D–H).

PCP increases brain functional connectivity in thalamic and fronto-hippocampal networks

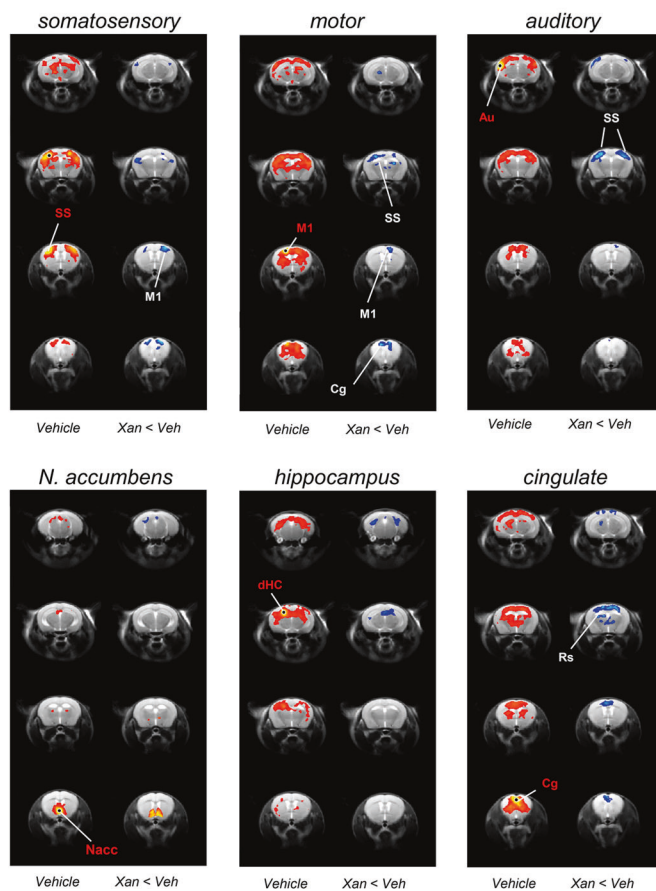
We next mapped foci of local and long-range (global) rsfMRI functional connectivity after PCP administration. Voxel-wise mapping revealed focally increased local connectivity in mid-brain/collicular regions of PCP-administered mice (Fig. 5A, C). A more widespread involvement of subcortical areas was apparent in long-range (global) connectivity maps, with prominent increases in thalamic and midbrain regions ($T > 3$, cluster corrected, Fig. 5A, D).

To elucidate the brain-wide network substrates affected by PCP, we used seed-based mapping to probe rsfMRI networks previously shown to be modulated by NMDAR antagonism in rodent studies [38]. Seed-based probing of polymodal cortical areas, the thalamus and ventral hippocampal highlighted widespread increases in functional connectivity in PCP-treated mice ($t > 2$, $p < 0.05$, cluster corrected, Fig. 5B). The most prominent effects were associated with the retrosplenial cortex and the thalamus, with PCP increasing connectivity between these substrates and extended cortical and subcortical networks. Notably, we also observed increased connectivity between the ventral

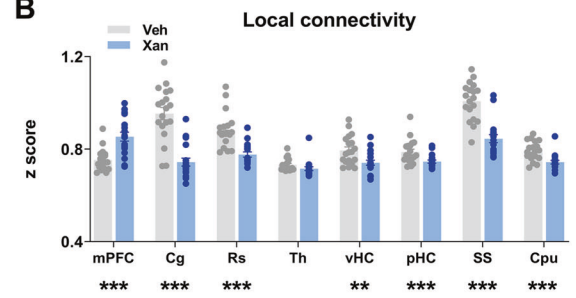
A



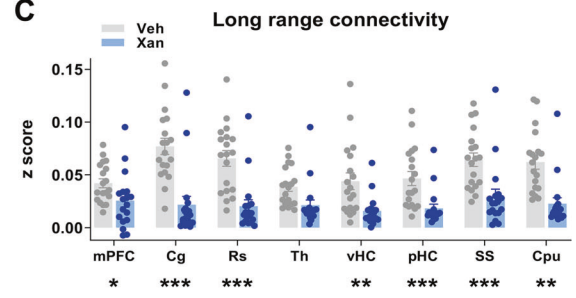
D



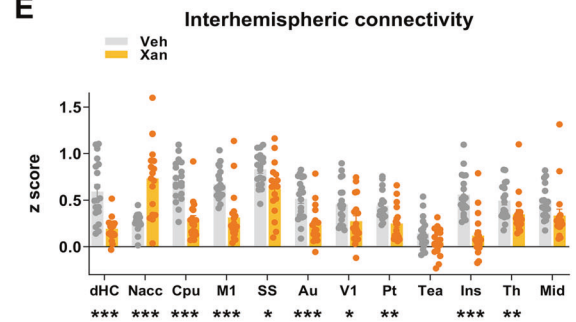
B



C



E



F

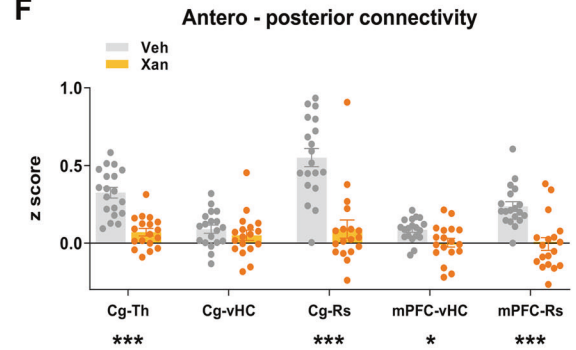


Fig. 2 Effect of xanomeline on functional connectivity in the mouse brain. A Contrast maps showing the difference in local (left) and long-range (right) connectivity between vehicle- and xanomeline-treated animals (one sample *t*-test, $t > \pm 3$, cluster corrected, Veh $N = 19$, Xan, $N = 18$). Blue reflects decreased connectivity, red reflects increased connectivity. **B, C** Quantification of local and long-range connectivity in selected brain volumes (mean \pm SEM, student *t* test, $*p < 0.05$, $**p < 0.01$, $***p < 0.001$, FDR corrected). **D–F** Xanomeline reduces long-range functional connectivity. **D** Seed-based mapping of selected rsfMRI networks. Network distribution in vehicle-treated controls is shown for reference (vehicle, $N = 19$). The effect of xanomeline ($N = 18$) is expressed as voxel-wise difference map with respect to vehicle group. Red/yellow indicates correlation with the seed regions ($t > \pm 3$, $p = 0.05$, cluster corrected). Blue indicates foci of reduced connectivity in the xanomeline group with respect to control group ($t > \pm 3$, $p = 0.05$, cluster corrected). Seed placements are indicated by dots and red lettering. **E** Pairwise functional connectivity between interhemispheric volumes of interest. Mean \pm SEM, $*p < 0.05$, $**p < 0.01$, $***p < 0.001$, Student *t* test, FDR corrected. **F** Pairwise functional connectivity between antero-posterior regions of interest. Mean \pm SEM, $*p < 0.05$, $**p < 0.01$, $***p < 0.001$, Student *t* test, FDR corrected. Au auditory cortex, pCtx parietal cortex, M1 primary motor cortex, NAcc nucleus accumbens, Ins insula, mPFC medial prefrontal cortex, Cg cingulate cortex, Rs retrosplenial cortex, Th thalamus, vHC ventral hippocampus, pHc posterior hippocampus, SS primary somatosensory cortex, CPU striatum, dHC dorsal hippocampus, V1 primary visual cortex, Pt posterior parietal association cortex, Tea temporal association cortex, Mid midbrain.

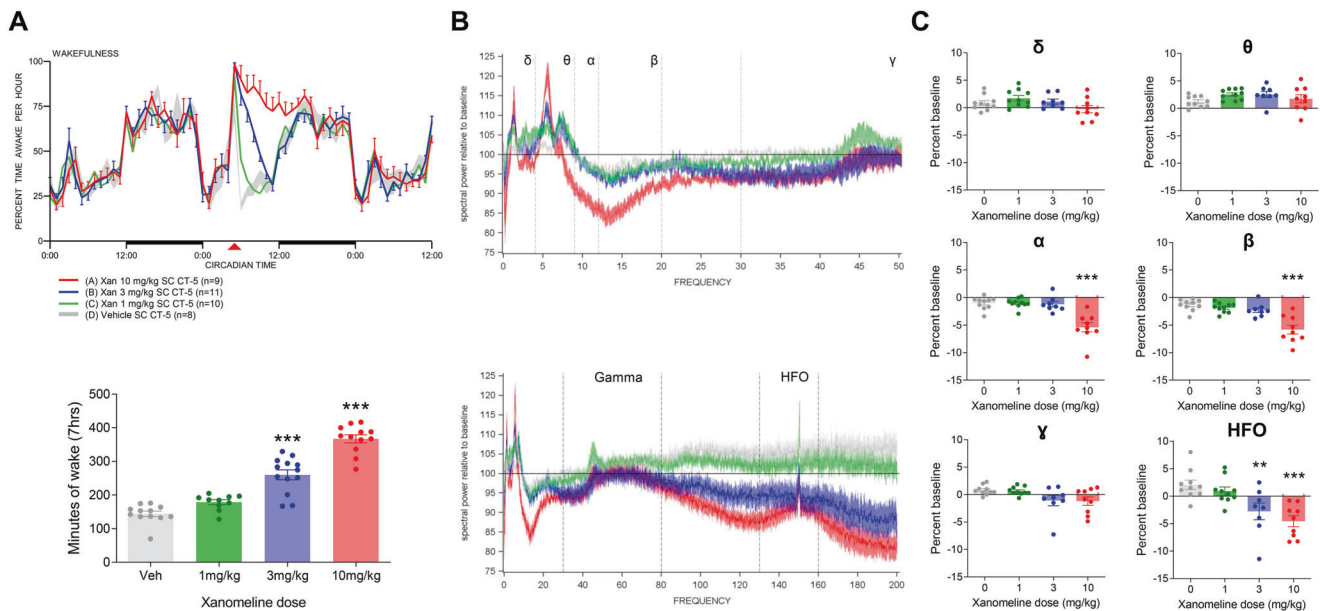


Fig. 3 Effect of xanomeline on sleep/wake and EEG spectral activity during wakefulness in the rat. Xanomeline increased wakefulness in a dose-dependent manner after s.c. administration. (A, top) Increased wakefulness (percent time awake per hour) was primarily over the first 7 h after dosing, returned to normal during the next dark period, and was significant at 3 and 10 mg/kg (A, bottom). Data are displayed as means \pm SEM ($***p < 0.001$, one-way ANOVA followed by Dunnett's test). B, C Waking spectral power during this 7 h period exhibited decreased alpha and beta power (B, top, 0–50 Hz range), unchanged gamma power (B, bottom, full frequency range) and decreased high-frequency oscillations (HFO) (B, bottom, full frequency range). Band-specific quantifications in (C) are expressed as percent change to vehicle control ($**p < 0.01$, $***p < 0.001$, Dunnett's test).

hippocampus and the prefrontal cortex, recapitulating similar findings produced by ketamine in the rat [38].

Xanomeline attenuates PCP-induced long-range connectivity alterations

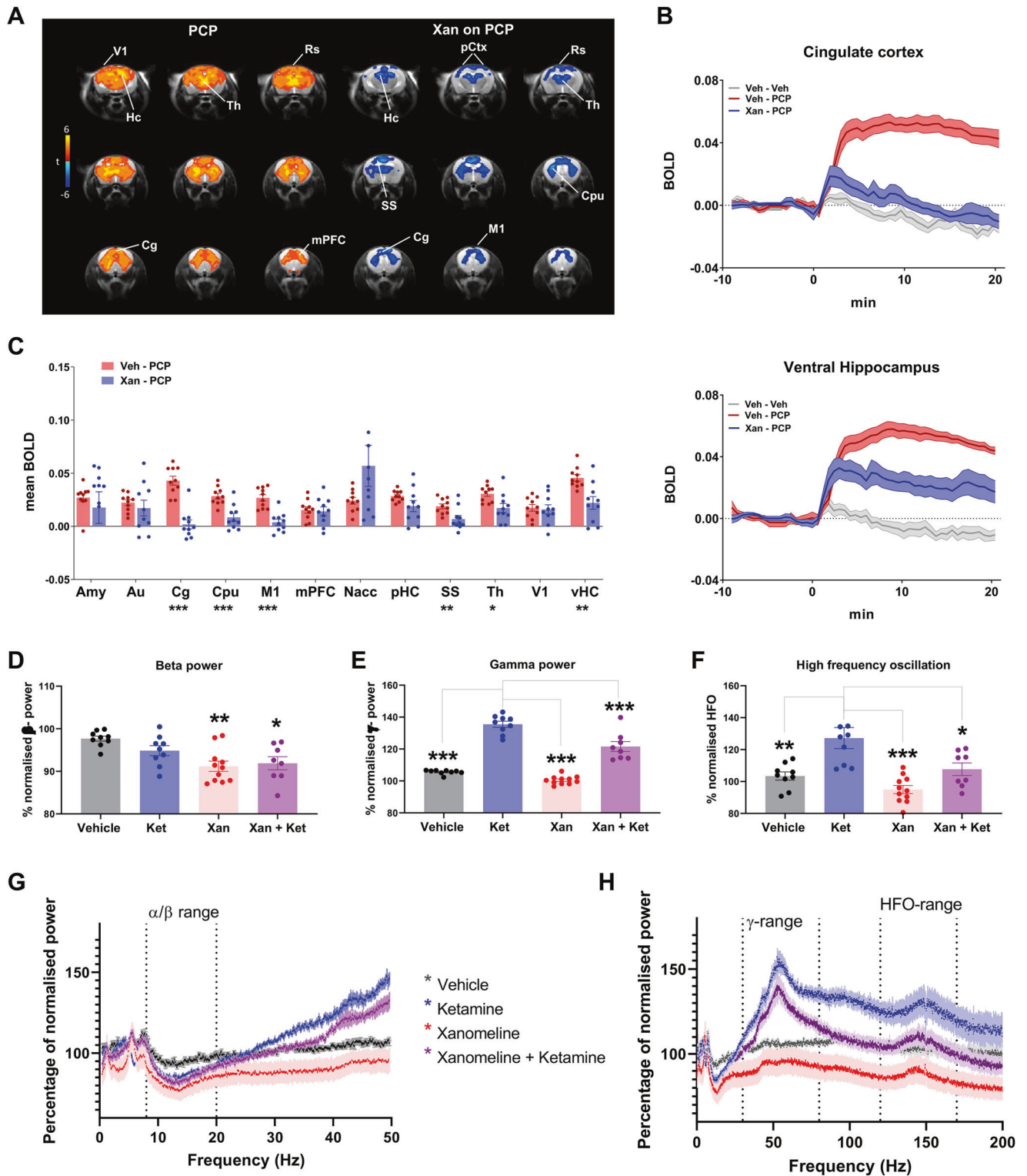
We next mapped the modulatory effect of xanomeline on PCP-induced local and long-range connectivity alterations by contrasting xanomeline-PCP with vehicle-PCP groups (Fig. 5E–I). Consistent with our prior mapping (cf. Fig. 2), xanomeline pretreatment in PCP challenged mice resulted in reduced local connectivity in cortical regions, but focally increased local connectivity in mesolimbic terminals like the nucleus accumbens. Interestingly, contrast maps for global connectivity showed evidence of reduced long-range connectivity in thalamic areas in xanomeline-pretreated animals, revealing the ability of the drug to prevent PCP-induced increases in thalamic global connectivity. Quantifications of these effect in regions of interest supported this interpretation, showing a reduction in PCP-induced thalamic long-range connectivity (Fig. 5G) in animals pretreated with xanomeline ($p < 0.05$, uncorrected), an effect that however did not survive FDR correction for multiple comparisons. A similar trend was observed in sensorimotor areas and in the retrosplenial cortex.

As above, we next interrogated these functional connectivity effects in specific functional networks using a seed-based approach (Fig. 5H, I). This analysis revealed that xanomeline pretreatment mitigated PCP-induced hyper-connectivity in several brain networks. Specifically, prominent foci of reduced connectivity in xanomeline-pretreated subjects were observed in thalamic and antero-posterior components of the mouse DMN, including fronto-hippocampal circuits. When quantified over large volumes of interest, a normalization of interhemispheric somatosensory connectivity was apparent in somatosensory areas, together with an increase in nucleus accumbens coupling in xanomeline-treated animals (Fig. 5I). Reduced antero-posterior cingulate-retrosplenial and fronto-hippocampal connectivity was also observed in xanomeline-pretreated animals (Fig. S5), with the former effect surviving FDR correction ($q < 0.05$).

DISCUSSION

Here we show that xanomeline acutely reduces functional connectivity in a widespread set of mouse brain networks and reverses the hyper-connectivity induced by PCP, but focally increasing connectivity in terminals of the mesolimbic pathway in both conditions. Moreover, our findings that xanomeline increases the BOLD signal across several neocortical regions (consistent with a cholinergic-stimulant action) and robustly suppresses PCP-induced pHfMRI-response, generalize previous findings with xanomeline, NMDAR antagonists and their interaction to the mouse. The corroboration of fMRI-derived hemodynamic measurements with EEG recordings of brain activity and amperometric measurements of brain oxygenation in non-sedated animals, underscores the robustness and substantiates a likely neural origin of the fMRI findings.

Agents that enhance cholinergic transmission have shown potential in improving cognitive function in individuals with AD and other memory disorders [54, 55]. The widespread BOLD signal increase observed with xanomeline in this study is consistent with a robust cholinergic-stimulant effect of the drug in mice, with similarly widespread increased pHfMRI signal reported in mice undergoing indirect stimulation of basal forebrain cholinergic pathways [56]. Our data also highlighted a significant widespread decrease in functional connectivity in xanomeline-treated animals. While the electrophysiological correlates of decreased rsfMRI synchronization are unknown, this effect is consistent with an increased cholinergic tone, which increases arousal and leads to neocortical disinhibition at timescales ranging from tens of milliseconds to many seconds [57]. It is therefore conceivable that the reduced neocortical rsfMRI connectivity may reflect a transition between slow, synchronized oscillations, to desynchronized, stochastic discharge that characterizes the awake/aroused state [58]. This finding adds to the weight of evidence regarding a possible beneficial action of this drug as a pro-cognitive agent in dementia or neurodegenerative disorders. Interestingly, in the ventro-medial prefrontal cortex and nucleus accumbens, xanomeline produced a local increase in functional connectivity. While the



origin and significance of this effect is unclear, it is interesting to note that the drug increases extracellular levels of dopamine and functional activation in the same regions [59].

A possible interpretational caveat that should be considered when pharmacological manipulations of the cholinergic systems are measured through hemodynamic readouts is a possible direct vascular effect of these drugs. Cholinergic modulators can affect the vasculature directly, with cholinergic agonists causing

vasodilatation and cholinergic antagonists vasoconstriction [60]. The administration of acetylcholine in muscarinic M5 knockout mice however did not produce any vasodilatation in the cerebral vasculature, suggesting that the M5 receptor subtype is responsible for vasoactive functions of acetylcholine in the brain [61, 62]. As xanomeline acts also as a partial agonist at the M5 receptor, a contribution of direct perivascular effects to the readouts mapped in our study cannot be entirely ruled out [63], although evidence

Fig. 4 Xanomeline effects on NMDAR antagonists in the mouse brain. **A** Left: Maps of BOLD response to PCP challenge (1 mg/Kg). Orange/yellow indicate increases in BOLD signal (veh-PCP vs. veh-veh, $Z > 4$, $p < 0.05$, cluster correction). Right: Contrast maps showing the xanomeline attenuation of PCP-induced fMRI activity (xan-PCP - veh-PCP, $Z > 3.1$, $p < 0.05$, cluster corrected). **B** Time course of BOLD signal in cingulate cortex (top) and ventral hippocampus (bottom). **C** BOLD response as quantified in volumes of interest, veh-PCP $n = 10$, xan-PCP = 10, mean \pm SEM, $*p < 0.05$, $**p < 0.01$, $***p < 0.001$, Student t test, FDR corrected (**D–H**). Xanomeline effects on ketamine-evoked EEG rat brain spectral activity. Power change in the EEG spectrum averaged over 6 h post dosing with drug or vehicle relative to an equivalent time-period 24 h earlier. **D, G** Effects in the 0–50 Hz range with similar drug evoked decreases in the alpha/beta range. **E, F, H** Effects across the full frequency range revealed increased gamma power and HFO with ketamine, and decreases in this range following pretreatment with Xanomeline. Veh ($n = 13$), Ket ($n = 10$), Xan ($n = 12$) Ket + Xan ($n = 15$). Data are displayed as means \pm SEM, $*p < 0.05$; $**p < 0.01$, $***p < 0.001$, one-way ANOVA followed by Dunnett's test. Significance in (**D**) is relative to veh, while in (**E**) and (**F**) significance is relative to ketamine alone. Hc hippocampus, Cg cingulate cortex, mPFC medial prefrontal cortex, Th thalamus, V1 primary visual cortex, vHC ventral hippocampus, Rs retrosplenial cortex, pCtx parietal cortex, CPu striatum, Amy amygdala, Au auditory cortex, M1 primary motor cortex, SS somatosensory cortex, SN substantia nigra, VTA ventral tegmental area, Nacc nucleus accumbens, pHc posterior hippocampus.

of the efficacy of xanomeline in counteracting the behavioral and neural effects of NMDAR antagonism strongly argue against a purely vascular effect of the mapped changes [64].

Xanomeline dosed 5 h into the light period of rats produced a pronounced increase in waking state, and a corresponding decrease in NREM and REM sleep as has been observed previously [65]. Similarly, EEG spectral activity during the waking vigilance state exhibited decreases in the alpha/beta range and while no change in gamma frequency was seen, a dose-dependent decrease in HFO (i.e., events recorded at frequencies higher than 80 Hz) was observed, recapitulating previous EEG findings in rats [65]. Importantly, HFO rhythms have been proposed as biomarker for pathological network activity [66, 67] and the ability of drugs to reduce these stimulations is considered as a putative biomarker of potential antipsychotic-like activity [65, 68, 69]. Preliminary investigations in AD patients suggest that the wake-promoting effects observed in rats might not appear to translate as potentially disruptive, as no significant change in normal sleep patterns were observed [13]. Further testing in healthy volunteers and other patient populations is warranted to assess the exact translational relevance of these findings. Prior investigations of xanomeline effects on sleep patterns have also examined interactions of this drug with noncompetitive NMDAR antagonists, revealing that xanomeline increased time awake and arousal during wake, but reduced slow wave activity during NREM sleep in rats [65]. This effect is of interest in the light of the emerging role of cholinergic activity in REM sleep (reviewed by [70]).

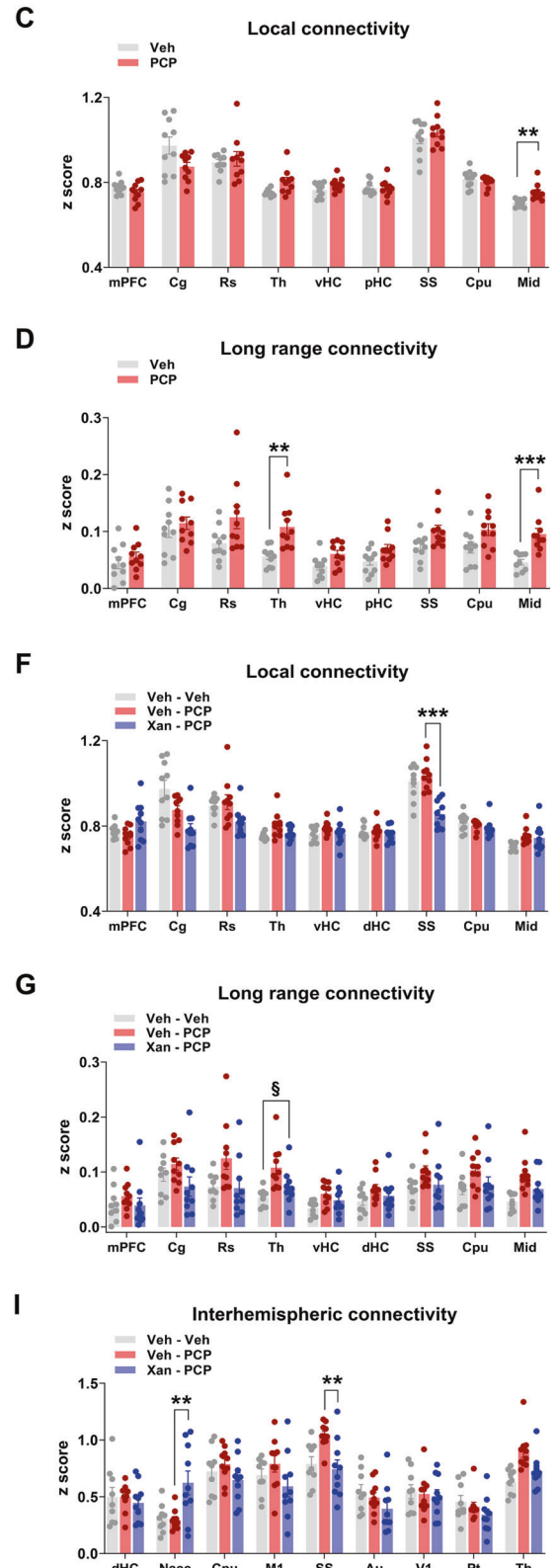
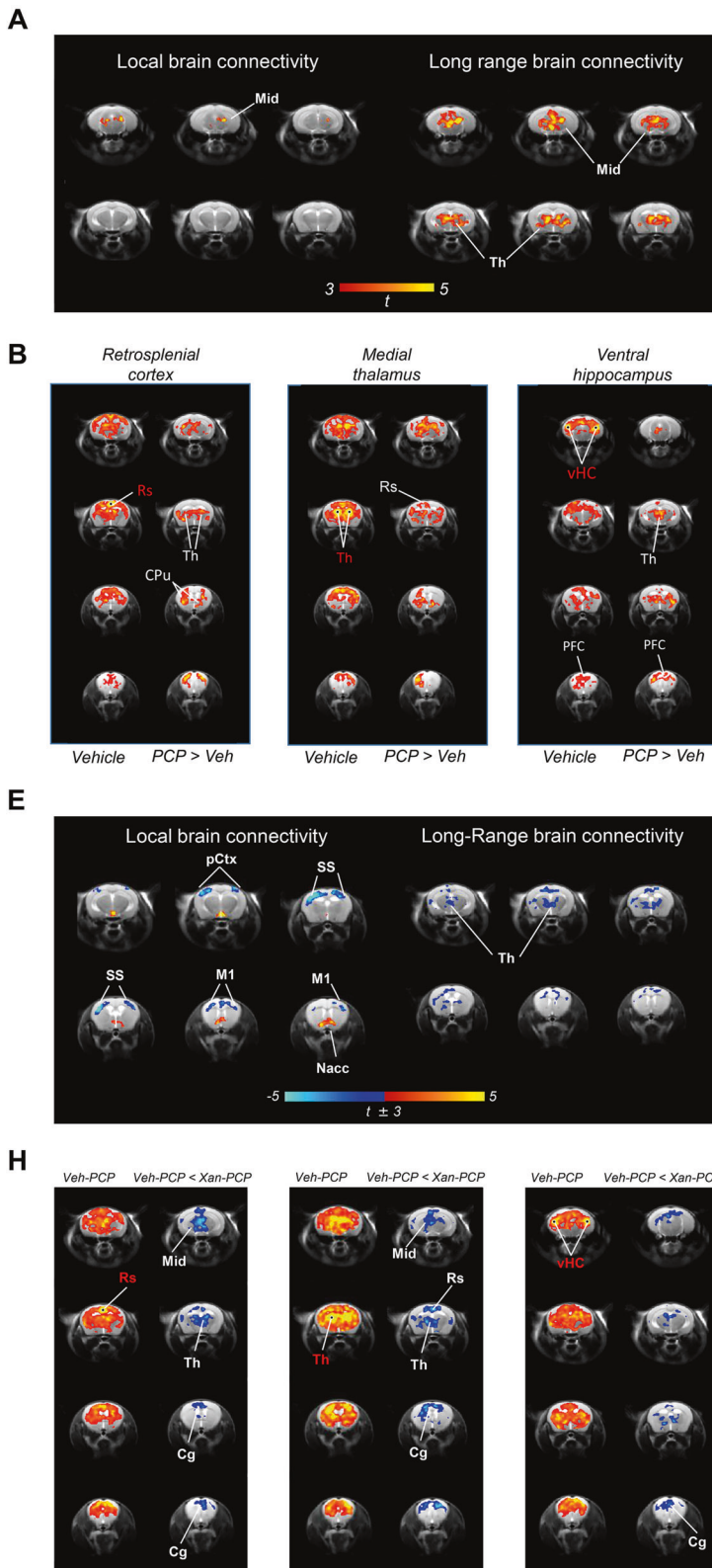
Human research has shown that subanesthetic doses of noncompetitive antagonists of NMDAR in healthy subjects [71], recapitulate cognitive impairments, negative symptoms, and brain functional abnormalities reminiscent of those mapped in schizophrenia [37, 72–75]. Both the univariate pHMRI response and multivariate rsfMRI network activity mapped upon PCP administration are consistent with the result of previous rodent and human mapping of NMDAR antagonism, most of which have been carried out with ketamine. Specifically, an increased in cortico–limbo–thalamic fMRI activity was previously shown in rats with PCP, and in humans with ketamine [26, 69, 75–77]. Moreover, reversal of the ketamine-evoked pHMRI response by pretreatment with two marketed compounds [26] and with novel glutamatergic agents [29] in humans indicates the potential utility of this approach as a translational CNS biomarker. Similarly, a thalamic increase in global (long-range) connectivity, as well as augmented fronto-hippocampal pairwise rsfMRI connectivity have been recently described in rodents and humans [38, 78–81]. Neural recordings corroborate these findings, providing evidence of increased interregional neural coherence after administration of NMDAR antagonists at different frequency ranges and between different brain areas, including the prefrontal-hippocampal axis [82–84]. It should however be noted that decreased cross-spectral density between PFC and dorsal hippocampus after ketamine administration has also been reported in freely behaving rats [85]. These results suggest that NMDAR modulation of

PFC-hippocampal coupling may exhibit subregional specificity, entailing increased coupling between directly innervated regions (i.e., PFC-ventral hippocampus), and nonlinear interactions in polymodally connected dorsal areas [86, 87].

Our observation that xanomeline can inhibit PCP-induced pHMRI response in anesthetized mice recapitulates the result of a previous fMRI characterization in awake rats [24], where the drug dose-dependently suppressed the effect of BOLD response to ketamine in widespread cortical areas [24]. This result corroborate the notion that light and controlled anesthesia only marginally affects the direction and qualitative patterns of spontaneous or evoked functional activity (see ref. [31] for a recent review). These findings also highlight consistent effects of xanomeline across rodent species, corroborating the translational robustness of the pHMRI. Establishing these responses in the mouse opens the way to interrogating brain functional changes in muscarinic-receptor knockout models with the aim to probe the functional role of specific muscarinic-receptor subtypes [88]. Moreover, knock-in of humanized muscarinic receptors could avoid dose-response bias due to the different characteristics of rodent and human muscarinic receptors [89].

Prior investigations using EEG recordings did not reveal any modulatory effect of xanomeline on the increased gamma activity produced by the selective NMDAR agonist MK-801 [65]. Here we report instead that xanomeline can effectively reduce the increase in high-frequency EEG activity produced by ketamine while having no effect on the reduction in lower frequency α/β activity. Interestingly the effects recorded were strongest in the HFO range. NMDAR antagonist evoked increases in HFO activity in nucleus accumbens have previously be shown to be reduced by clozapine [68]. The ketamine-induced power changes in β -power and γ -power observed here and in other preclinical studies [52] have been recapitulated in humans [53] and correlated with fMRI connectivity changes [34]. However, HFO activity has not yet been reported in humans. The ability of xanomeline to decrease the functional effects of PCP and ketamine is therefore consistent with a putative antipsychotic action of this compound.

A number of other recent studies have shown the ability of various acetylcholinergic modulators to modulate brain imaging and electrophysiology signals. The muscarinic acetylcholine receptor antagonist scopolamine caused functional connectivity disruption in cingulate and prefrontal regions of the mouse brain, an effect recovered by the muscarinic agonist milameline [90]. These rsfMRI results data are directionally consistent with the functional desynchronization we observed with xanomeline, despite the seemingly divergent pharmacological profile (antagonist vs. agonist) of these two compounds. Given the complex pre- and post-synaptic distribution of muscarinic receptors, it is however unclear whether scopolamine functionally silences or increases cortical cholinergic tone. In rats, the M4-selective PAM VU0152100 blocked both the pHMRI response and striatal dopamine release induced by amphetamine alone [91]. In contrast, VU0152100 per se had no significant effect on either



measure. The M1-selective PAM TAK-071 was shown to attenuate alpha and theta power increases on qEEG elicited by scopolamine in cynomolgous monkeys. The same study also examined xanomeline and the acetylcholinesterase inhibitor donepezil as comparators [92]. In that study, 1 mg/kg xanomeline did not significantly modulate the qEEG signals whereas 3 mg/kg

donepezil attenuated only the delta band power increase. The selective M1 antagonist biperiden was studied using rsfMRI in healthy human volunteers as well as medication-free individuals with psychotic disorders, showing a trend to increased functional connectivity in the frontal cortex [93]. These effects with more selective molecules are broadly and directionally consistent with

Fig. 5 Effect of PCP on functional connectivity, and its antagonization by xanomeline. A–D PCP increases brain functional connectivity. **A** Effect of PCP on global and local brain connectivity. Red/yellow reflects increase in connectivity strength ($t > 3$, $p < 0.05$, cluster correction; Veh, $N = 9$; PCP $N = 10$). **B** Seed–correlation mapping highlighted increased connectivity in cortical and subcortical networks of PCP-treated animals. On the left column of each panel, correlation with the seed of interest is reported for vehicle-treated animals ($n = 9$; $t > 2.7$, $p < 0.05$, cluster corrected). The right column of each panel indicates the corresponding connectivity difference in PCP-treated animals (red/yellow indicates connectivity increase in PCP-treated group with respect to control, $z > 2$; veh, $n = 9$; PCP, $n = 10$; $p < 0.05$, cluster corrected). **C–D** Quantification of Local connectivity and long-range connectivity in selected brain regions (mean \pm SEM, student t test, $**p < 0.01$, FDR corrected). **E–I** Xanomeline attenuates PCP-induced long-range functional connectivity changes in the mouse brain. **E** Modulatory effect of xanomeline on PCP-induced local and global connectivity (Xan-PCP vs. veh-PCP, $t \pm 3$, $p < 0.05$, cluster corrected). **F, G** Quantification of local connectivity and long-range connectivity in volumes of interest (mean \pm SEM, student t test, xan-PCP vs. veh-PCP, $***p < 0.01$, FDR corrected; $^{\circ}p < 0.05$, uncorrected). **H** Seed-based probing of rsfMRI networks. On the left column of each panel, correlation with the seed of interest is reported for control (vehicle pretreated) subjects ($N = 9$; $t > 2.7$, $p < 0.05$, cluster corrected). The right column of each panel indicates the corresponding connectivity difference in xanomeline-pretreated animals (blue indicates significant connectivity decrease in xanomeline-PCP group ($N = 10$) with respect to control vehicle-PCP, ($N = 10$) $Z > 2$, $p < 0.05$, cluster corrected). **I** Quantification of interhemispheric rsfMRI connectivity (mean \pm SEM, student t test, xan-PCP vs. veh-PCP. $**p < 0.01$, FDR corrected). Au auditory cortex, mPFC medial prefrontal cortex, Cg cingulate cortex, Rs retrosplenial cortex, Th thalamus, vHC ventral hippocampus, SS primary, somatosensory cortex, CPu striatum, Mid midbrain, pCtx parietal cortex, M1 primary motor cortex, Nacc nucleus accumbens, dHC dorsal hippocampus. PFC prefrontal cortex, pHc posterior hippocampus, V1 primary visual cortex, Pt posterior parietal association cortex.

those reported in the current study, showing that activation of M1 and M4 receptors can partially normalize aberrant brain activity—using hemodynamic, electrophysiological, or pharmacological readouts—induced by amphetamine [91], scopolamine [92] and PCP or ketamine (this study). In contrast, the human data with the M1 antagonist showed a trend toward increased functional connectivity, directionally opposed to the decreased functional connectivity elicited by xanomeline in the present study.

A recent study has described a pharmacokinetic assessment of xanomeline in the mouse brain, allowing the *in vivo* engagement of the drug at different receptor subtypes to be estimated [5]. This investigation revealed that the highest xanomeline dose tested here (30 mg/kg) would result in an unbound drug fraction that is almost 10-fold and 40-fold higher than the M1 and M4 EC_{50} values, respectively, and on the same order of magnitude of human M2, M3, and M5 EC_{50} . While these values corroborate the notion that M4 and M1 receptors are the most plausible drivers of the behavioral and functional changes mapped in our work, a non-negligible contribution from M2, M3, and M5 muscarinic receptors cannot be entirely ruled out at the highest dose tested here. Further investigations with more selective new-generation muscarinic drugs [91–93] are warranted to dissect the relative functional and pharmacological contribution of each receptor subtypes.

A few additional technical limitations in our study deserve to be mentioned. First, some of the studies reported here were carried out at different times and different institutions, and only retrospectively assembled. As a result of this, inconsistencies in the rodent species and strain used (e.g., rat vs. mouse), NMDAR antagonists tested (e.g., PCPC vs. ketamine), xanomeline doses and routes of administration employed, and availability of plasma exposure data were present, providing an important caveat to directly comparing the efficacy of the drug across assays. Moreover, while our results can enhance clinical translation and the identification of reliable biomarkers sensitive to cholinergic modulations, the exact clinical relevance of our imaging results remains unclear, and their clinical extrapolation should be exercised with great caution owing to our poor understanding of the causal or epiphenomenal nature of functional connectivity in brain disorders [94], and our limited knowledge of the neural basis of brain-wide coupling [95].

In conclusion, our data document that the M1/M4 preferring muscarinic agonist xanomeline induces a widespread pHMRI response and decreases functional connectivity in the mouse brain. Moreover, xanomeline also reverses the functional and connectivity effects induced by NMDAR antagonists ketamine and PCP. These results are consistent with a putative anti-psychotic profile of this drug, and suggest EEG, pHMRI, and/or rsfMRI as potentially useful pharmacodynamic biomarkers for

the determination of central biological activity in human clinical studies.

FUNDING AND DISCLOSURE

This study was funded by Eli-Lilly. The authors declare no competing interests.

AUTHOR CONTRIBUTIONS

Conceptualization, AG, AS, GG, and CF; data acquisition and analysis, AGa, CC, CM, AM, DS, KK, JL, KW, DG-B, and DM; writing—original draft, AG; writing—review/edit, AG, AS, CF, CM; supervision, AG, CF, and AS.

ADDITIONAL INFORMATION

Supplementary Information accompanies this paper at (<https://doi.org/10.1038/s41386-020-00916-0>).

Publisher's note Springer Nature remains neutral with regard to jurisdictional claims in published maps and institutional affiliations.

REFERENCES

- Shannon HE, Rasmussen K, Bymaster FP, Hart JC, Peters SC, Swedberg MDB, et al. Xanomeline, an M1/M4 preferring muscarinic cholinergic receptor agonist, produces antipsychotic-like activity in rats and mice. *Schizophr Res.* 2000;42:249–59. [https://doi.org/10.1016/S0920-9964\(99\)00138-3](https://doi.org/10.1016/S0920-9964(99)00138-3)
- Andersen MB, Fink-Jensen A, Peacock L, Gerlach J, Bymaster F, Lundbaek JA, et al. The muscarinic M1/M4 receptor agonist xanomeline exhibits antipsychotic-like activity in Cebus apella monkeys. *Neuropsychopharmacology.* 2003;28:1168–75. <https://doi.org/10.1038/sj.npp.1300151>
- Mirza NR, Peters D, Sparks RG. Xanomeline and the antipsychotic potential of muscarinic receptor subtype selective agonists. *CNS Drug Rev.* 2003;9:159–86. <https://doi.org/10.1111/j.1527-3458.2003.tb00247.x>
- Martino G, Puma C, Yu XH, Gilbert AK, Coupal M, Markoglou N, et al. The M1/M4 preferring agonist xanomeline is analgesic in rodent models of chronic inflammatory and neuropathic pain via central site of action. *Pain.* 2011;152:2852–60. <https://doi.org/10.1016/j.pain.2011.09.017>
- Thorn CA, Moon J, Bourbonais CA, Harms J, Edgerton JR, Stark E, et al. Striatal, Hippocampal, And Cortical Networks Are Differentially Responsive to the M4- and M1-muscarinic acetylcholine receptor mediated effects of xanomeline. *ACS Chem Neurosci.* 2019;10:1753–64. <https://doi.org/10.1021/acscchemneuro.8b00625>
- Picciotto MR, Higley MJ, Mineur YS. Acetylcholine as a neuromodulator: cholinergic signaling shapes nervous system function and behavior. *Neuron.* 2012;76:116–29. <https://doi.org/10.1016/j.neuron.2012.08.036>
- Moran SP, Maksymetz J, Conn PJ. Targeting muscarinic acetylcholine receptors for the treatment of psychiatric and neurological disorders. *Trends Pharmacol Sci.* 2019;40:1006–20. <https://doi.org/10.1016/j.tips.2019.10.007>
- Verma S, Kumar A, Tripathi T, Kumar A. Muscarinic and nicotinic acetylcholine receptor agonists: current scenario in Alzheimer's disease therapy. *J Pharm Pharmacol.* 2018;70:985–93. <https://doi.org/10.1111/jphp.12919>

9. Felder CC, Goldsmith PJ, Jackson K, Sanger HE, Evans DA, Mogg AJ, et al. Current status of muscarinic M1 and M4 receptors as drug targets for neurodegenerative diseases. *Neuropharmacology*. 2018;136:449–58. <https://doi.org/10.1016/j.neuropharm.2018.01.028>
10. Erskine D, Taylor J-P, Bakker G, Brown AJH, Tasker T, Nathan PJ. Cholinergic muscarinic M1 and M4 receptors as therapeutic targets for cognitive, behavioural, and psychological symptoms in psychiatric and neurological disorders. *Drug Discov Today*. 2019;24:2307–14. <https://doi.org/10.1016/j.drudis.2019.08.009>
11. Melancon BJ, Tarr JC, Panarese JD, Wood MR, Lindsley CW. Allosteric modulation of the M1 muscarinic acetylcholine receptor: improving cognition and a potential treatment for schizophrenia and Alzheimer's disease. *Drug Discov Today*. 2013;18:1185–99. <https://doi.org/10.1016/j.drudis.2013.09.005>
12. Avery EE, Baker LD, Asthana S. Potential role of muscarinic agonists in Alzheimer's Disease. *Drugs Aging*. 1997;11:450–9. <https://doi.org/10.2165/00002512-199711060-00004>
13. Bodick NC, Offen WW, Levey AI, Cutler NR, Gauthier SG, Satlin A, et al. Effects of xanomeline, a selective muscarinic receptor agonist, on cognitive function and behavioral symptoms in Alzheimer disease. *Arch Neurol*. 1997;54:465–73. <https://doi.org/10.1001/archneur.1997.00550160091022>
14. Cui YH, Si W, Yin L, An SM, Jin J, Deng SN, et al. A novel derivative of xanomeline improved memory function in aged mice. *Neurosci Bull*. 2008;24:251–7. <https://doi.org/10.1007/s12264-008-0204-5>
15. W Si, X Zhang, Y Niu, H Yu, X Lei, H Chen, et al. A novel derivative of xanomeline improves fear cognition in aged mice, 2010. <https://doi.org/10.1016/j.neulet.2010.02.031>
16. D Wang, L Yang, J Su, Y Niu, X Lei, J Xiong, et al. Attenuation of neurodegenerative phenotypes in Alzheimer-like presenilin 1/presenilin 2 conditional double knockout mice by EUK1001, a promising derivative of xanomeline, 2011. <https://doi.org/10.1016/j.bbrc.2011.05.120>
17. Sullivan RJ, Allen JS, Otto C, Tiobech J, Nero K. Effects of chewing betel nut (*Arecatechu*) on the symptoms of people with schizophrenia in Palau, Micronesia. *Br J Psychiatry*. 2000;177:174–8. <https://doi.org/10.1192/bjp.177.2.174>
18. Scarr E, Dean B. Muscarinic receptors: Do they have a role in the pathology and treatment of schizophrenia? *J Neurochem*. 2008;107:1188–95. <https://doi.org/10.1111/j.1471-4159.2008.05711.x>
19. Shannon HE, Hart JC, Bymaster FP, Calligaro DO, Delapp NW, Mitch CH, et al. Muscarinic receptor agonists, like dopamine receptor antagonist antipsychotics, inhibit conditioned avoidance response in rats. *J Pharmacol Exp Ther*. 1999;290:901–7.
20. Stanhope KJ, Mirza NR, Bickerdike MJ, Bright JL, Harrington NR, Hesselink MB, et al. The muscarinic receptor agonist xanomeline has an antipsychotic-like profile in the rat. *J Pharmacol Exp Ther*. 2001;299:782–92.
21. Shekhar A, Potter WZ, Lightfoot J, Lienemann J, Dub S, Mallinckrodt C, et al. Selective muscarinic receptor agonist xanomeline as a novel treatment approach for schizophrenia. *Am J Psychiatry*. 2008;165:1033–9. <https://doi.org/10.1176/appi.ajp.2008.06091591>
22. Raedler TJ, Bymaster FP, Tandon R, Copolov D, Dean B. Towards a muscarinic hypothesis of schizophrenia. *Mol Psychiatry*. 2007;12:232–46. <https://doi.org/10.1038/sj.mp.4001924>
23. Langmead CJ, Watson J, Reavill C. Muscarinic acetylcholine receptors as CNS drug targets. *Pharmacol Ther*. 2008;117:232–43. <https://doi.org/10.1016/j.pharmthera.2007.09.009>
24. Baker S, Chin CL, Basso AM, Fox GB, Marek GJ, Day M. Xanomeline modulation of the blood oxygenation level-dependent signal in awake rats: development of pharmacological magnetic resonance imaging as a translatable pharmacodynamic biomarker for central activity and dose selection. *J Pharmacol Exp Ther*. 2012;341:263–73. <https://doi.org/10.1124/jpet.111.188797>
25. De Simoni S, Schwarz AJ, O'Daly OG, Marquand AF, Brittain C, Gonzales C, et al. Test-retest reliability of the BOLD pharmacological MRI response to ketamine in healthy volunteers. *Neuroimage*. 2013;64:75–90.
26. Doyle OM, De Simoni S, Schwarz AJ, Brittain C, O'Daly OG, Williams SCR, et al. Quantifying the attenuation of the ketamine pharmacological magnetic resonance imaging response in humans: a validation using antipsychotic and glutamatergic agents. *J Pharmacol Exp Ther*. 2013;345:151–60.
27. Javitt DC, Carter CS, Krystal JH, Kantrowitz JT, Girgis RR, Kegeles LS, et al. Utility of imaging-based biomarkers for glutamate-targeted drug development in psychotic disorders: a randomized clinical trial. *JAMA Psychiatry*. 2018;75:11–19. <https://doi.org/10.1001/jamapsychiatry.2017.3572>
28. Javitt DC, Lee M, Kantrowitz JT, Martinez A. Mismatch negativity as a biomarker of theta band oscillatory dysfunction in schizophrenia. *Schizophr Res*. 2018;191:51–60. <https://doi.org/10.1016/j.schres.2017.06.023>
29. Mehta MA, Schmechtig A, Kotoula V, McColm J, Jackson K, Brittain C, et al. Group II metabotropic glutamate receptor agonist prodrugs LY2979165 and LY2140023 attenuate the functional imaging response to ketamine in healthy subjects. *Psychopharmacology*. 2018;235:1875–86. <https://doi.org/10.1007/s00213-018-4877-9>
30. Errico F, D'Argenio V, Sforzini F, Iasevoli F, Squillace M, Guerri G, et al. A role for D-aspartate oxidase in schizophrenia and in schizophrenia-related symptoms induced by phencyclidine in mice. *Transl Psychiatry*. 2015;5:e512. <https://doi.org/10.1038/tp.2015.2>
31. Gozzi A, Schwarz AJ. Large-scale functional connectivity networks in the rodent brain. *Neuroimage*. 2016;127:496–509. <https://doi.org/10.1016/j.neuroimage.2015.12.017>
32. Lowry JP, Boutelle MG, Fillenz M. Measurement of brain tissue oxygen at a carbon paste electrode can serve as an index of increases in regional cerebral blood flow. *J Neurosci Methods*. 1997;71:177–82. [https://doi.org/10.1016/S0165-0270\(96\)00140-9](https://doi.org/10.1016/S0165-0270(96)00140-9)
33. Li J, Schwarz AJ, Gilmour G. Relating translational neuroimaging and amperometric endpoints: utility for neuropsychiatric drug discovery. *Curr Top Behav Neurosci*. 2016;28:397–421. https://doi.org/10.1007/7854_2016_1
34. Zacharias N, Musso F, Müller F, Lammers F, Saleh A, London M, et al. Ketamine effects on default mode network activity and vigilance: a randomized, placebo-controlled crossover simultaneous fMRI/EEG study. *Hum Brain Mapp*. 2020;41:107–19. <https://doi.org/10.1002/hbm.24791>
35. Ye T, Bartlett MJ, Schmit MB, Sherman SJ, Falk T, Cowen SL. Ten-hour exposure to low-dose ketamine enhances corticostriatal cross-frequency coupling and hippocampal broad-band gamma oscillations. *Front Neural Circuits*. 2018;12:61. <https://doi.org/10.3389/fncir.2018.00061>
36. Greene R. Circuit analysis of NMDAR hypofunction in the hippocampus, in vitro, and psychosis of schizophrenia. *Hippocampus*. 2001;11:569–77. <https://doi.org/10.1002/hipo.1072>
37. Farber NB. The NMDA receptor hypofunction model of psychosis. *Ann N Y Acad Sci*. 2003;1003:119–30.
38. Gass N, Schwarz AJ, Sartorius E, Schenker E, Risterucci C, Spedding L, et al. Sub-anesthetic ketamine modulates intrinsic BOLD connectivity within the hippocampal-prefrontal circuit in the rat. *Neuropsychopharmacology*. 2013;39:895–906.
39. Gozzi A, Large C, Schwarz A, Bertani S, Crestan V, Bifone A. Differential effects of antipsychotic and glutamatergic agents on the pHMRI response to phencyclidine. *Neuropsychopharmacology*. 2008;33:1690–703.
40. Gozzi A, Schwarz A, Crestan V, Bifone A. Drug-anesthetic interaction in pHMRI: the case of the psychotomimetic agent phencyclidine. *Magn Reson Imaging*. 2008;26:999–1006. <https://doi.org/10.1016/j.mri.2008.01.012>
41. Gozzi A, Herdon H, Schwarz A, Bertani S, Crestan V, Turrini G, et al. Pharmacological stimulation of NMDA receptors via co-agonist site suppresses fMRI response to phencyclidine in the rat. *Psychopharmacology*. 2008;201:273–84. <https://doi.org/10.1007/s00213-008-1271-z>
42. Li J, Ishiwari K, Conway MW, Francois J, Huxter J, Lowry JP, et al. Dissociable effects of antipsychotics on ketamine-induced changes in regional oxygenation and inter-regional coherence of low frequency oxygen fluctuations in the rat. *Neuropsychopharmacology*. 2014;39:1635–44. <https://doi.org/10.1038/npp.2014.10>
43. Watt ML, Rorick-Kehn L, Shaw DB, Knitowski KM, Quets AT, Chesterfield AK, et al. The muscarinic acetylcholine receptor agonist BuTAC mediates antipsychotic-like effects via the M4 subtype. *Neuropsychopharmacology*. 2013;38:2717–26. <https://doi.org/10.1038/npp.2013.186>
44. Ferrari L, Turrini G, Crestan V, Bertani S, Cristofori P, Bifone A, et al. A robust experimental protocol for pharmacological fMRI in rats and mice. *J Neurosci Methods*. 2012;204:9–18. <https://doi.org/10.1016/j.jneumeth.2011.10.020>
45. Sforzini F, Schwarz AJ, Galbusera A, Bifone A, Gozzi A. Distributed BOLD and CBV-weighted resting-state networks in the mouse brain. *Neuroimage*. 2014;87:403–15. <https://doi.org/10.1016/j.neuroimage.2013.09.050>
46. Zhan Y, Paolicelli RC, Sforzini F, Weinhart L, Bolasco G, Pagani F, et al. Deficient neuron-microglia signaling results in impaired functional brain connectivity and social behavior. *Nat Neurosci*. 2014;17:400–6. <https://doi.org/10.1038/nn.3641>
47. Bertani S, Carboni L, Criado A, Michielin F, Mangiarini L, Vicentini E. Circadian profile of peripheral hormone levels in Sprague-Dawley rats and in common marmosets (*Callithrix jacchus*). *Vivo*. 2010;24:827–36.
48. Seidel WF, Maze M, Dement WC, Edgar DM. Alpha-2 adrenergic modulation of sleep: time-of-day-dependent pharmacodynamic profiles of dexmedetomidine and clonidine in the rat. *J Pharmacol Exp Ther*. 1995;275:263–73.
49. Van Gelder RN, Edgar DM, Dement WC. Real-time automated sleep scoring: validation of a microcomputer-based system for mice. *Sleep*. 1991;14:48–55. <https://doi.org/10.1093/sleep/14.1.48>
50. Gozzi A, Ceolin L, Schwarz A, Reese T, Bertani S, Crestan V, et al. A multimodality investigation of cerebral hemodynamics and autoregulation in pharmacological MRI. *Magn Reson Imaging*. 2007;25:826–33. <https://doi.org/10.1016/j.mri.2007.03.003>
51. Liska A, Bertero A, Gomolka R, Sabbioni M, Galbusera A, Barsotti N, et al. Homozygous loss of autism-risk gene CNTNAP2 results in reduced local and long-

- range prefrontal functional connectivity, Homozygous Loss Autism-Risk Gene *Cntnap2* Results Reduc. Local Long-Range Prefrontal Funct. Connect. 2016;060335. <https://doi.org/10.1101/060335>
52. Phillips KG, Cotel MC, McCarthy AP, Edgar DM, Tricklebank M, O'Neill MJ, et al. Differential effects of NMDA antagonists on high frequency and gamma EEG oscillations in a neurodevelopmental model of schizophrenia. *Neuropharmacology*. 2012;62:1359–70. <https://doi.org/10.1016/j.neuropharm.2011.04.006>
53. Muthukumaraswamy SD, Shaw AD, Jackson LE, Hall J, Moran R, Saxena N. Evidence that subanesthetic doses of ketamine cause sustained disruptions of NMDA and AMPA-mediated frontoparietal connectivity in humans. *J Neurosci*. 2015;35:11694–706. <https://doi.org/10.1523/JNEUROSCI.0903-15.2015>
54. Green MF, Kern RS, Braff DL, Mintz J. Neurocognitive deficits and functional outcome in schizophrenia: are we measuring the “right stuff”? *Schizophr Bull*. 2000;26:119.
55. Green MF, Kern RS, Heaton RK. Longitudinal studies of cognition and functional outcome in schizophrenia: implications for MATRICS. *Schizophr Res*. 2004;72:41–51.
56. Gozzi A, Apar J, Giovannelli A, Bertolini C, Crestan V, Schwarz AJ, et al. A neural switch for active and passive fear. *Neuron*. 2010;67:656–66.
57. Poorthuis RB, Enke L, Letzkus JJ. Cholinergic circuit modulation through differential recruitment of neocortical interneuron types during behaviour. *J Physiol*. 2014;592:4155–64. <https://doi.org/10.1113/jphysiol.2014.273862>
58. Lawrence JJ. Cholinergic control of GABA release: emerging parallels between neocortex and hippocampus. *Trends Neurosci*. 2008;31:317–27. <https://doi.org/10.1016/j.tins.2008.03.008>
59. Perry KW, Nisenbaum LK, George CA, Shannon HE, Felder CC, Bymaster FP. The muscarinic agonist xanomeline increases monoamine release and immediate early gene expression in the rat prefrontal cortex. *Biol Psychiatry*. 2001;49:716–25. [https://doi.org/10.1016/S0006-3223\(00\)01017-9](https://doi.org/10.1016/S0006-3223(00)01017-9)
60. Sato A, Sato Y. Cholinergic neural regulation of regional cerebral blood flow. *Alzheimer Dis Assoc Disord*. 1995;9:28–38. <https://doi.org/10.1097/00002093-199505000-00007>
61. Yamada M, Lamping KG, Duttaroy A, Zhang W, Cui Y, Bymaster FP, et al. Cholinergic dilation of cerebral blood vessels is abolished in M5 muscarinic acetylcholine receptor knockout mice. *Proc Natl Acad Sci*. 2001;98:14096–101.
62. Yamada M, Basile AS, Fedorova I, Zhang W, Duttaroy A, Cui Y, et al. Novel insights into M5 muscarinic acetylcholine receptor function by the use of gene targeting technology. *Life Sci*. 2003;74:345–53.
63. Grant MKO, El-Fakahany EE. Persistent binding and functional antagonism by xanomeline at the muscarinic M5 receptor. *J Pharmacol Exp Ther*. 2005;315:313–9. <https://doi.org/10.1124/jpet.105.090134>
64. Barak S, Weiner I. The M1/M4 preferring agonist xanomeline reverses amphetamine-, MK801- and scopolamine-induced abnormalities of latent inhibition: putative efficacy against positive, negative and cognitive symptoms in schizophrenia. *Int J Neuropsychopharmacol*. 2011;14:1233–46. <https://doi.org/10.1017/S1461145710001549>
65. Gould RW, Nedelcovych MT, Gong X, Tsai E, Bubser M, Bridges TM, et al. State-dependent alterations in sleep/wake architecture elicited by the M4 PAM VU0467154 - Relation to antipsychotic-like drug effects. *Neuropharmacology*. 2016;202:244–53. <https://doi.org/10.1016/j.neuropharm.2015.11.016>
66. Kucewicz MT, Cimbalnik J, Matsumoto JY, Brinkmann BH, Bower MR, Vasoli V, et al. High frequency oscillations are associated with cognitive processing in human recognition memory. *A J. Neurol*. <https://doi.org/10.1093/brain/awu149>
67. Jacob S, Davies G, De Bock M, Hermans B, Wintmolders C, Bittelbergs A, et al. Neural oscillations during cognitive processes in an App knock-in mouse model of Alzheimer's disease pathology. *Sci Rep*. 2019;9:16363 <https://doi.org/10.1038/s41598-019-51928-w>
68. Hunt MJ, Olszewski M, Piasecka J, Whittington MA, Kasicki S. Effects of NMDA receptor antagonists and antipsychotics on high frequency oscillations recorded in the nucleus accumbens of freely moving mice. *Psychopharmacology*. 2015;232:4525–35. <https://doi.org/10.1007/s00213-015-4073-0>
69. Becker R, Braun U, Schwarz AJ, Gass N, Schweiger JI, Weber-Fahr W, et al. Species-conserved reconfigurations of brain network topology induced by ketamine. *Transl Psychiatry*. 2016;6:e786 <https://doi.org/10.1038/tp.2016.53>
70. Yamada RG, Ueda HR. Molecular mechanisms of REM sleep. *Front Neurosci*. 2020;13:1402 <https://doi.org/10.3389/fnins.2019.01402>
71. Anis NA, Berry SC, Burton NR, Lodge D. The dissociative anaesthetics, ketamine and phencyclidine, selectively reduce excitation of central mammalian neurones by N-methyl-aspartate. *Br J Pharm*. 1983;79:565–75. <https://doi.org/10.1111/j.1476-5381.1983.tb11031.x>
72. Coyle JT, Tsai G, Goff D. Converging evidence of NMDA receptor hypofunction in the pathophysiology of schizophrenia. *Ann N. Y Acad Sci*. 2003;1003:318–27. <https://doi.org/10.1196/annals.1300.020>
73. Moghaddam B, Jackson ME. Glutamatergic animal models of schizophrenia. *Ann N. Y Acad Sci*. 2003;1003:131–7.
74. Adler CM, Malhotra AK, Elman I, Goldberg T, Egan M, Pickar D, et al. Comparison of ketamine-induced thought disorder in healthy volunteers and thought disorder in schizophrenia. *Am J Psychiatry*. 1999;156:1646–9.
75. Schwarz AJ, Gozzi A, Reese T, Heidbreder CA, Bifone A. Pharmacological modulation of functional connectivity: the correlation structure underlying the pHMRI response to d-amphetamine modified by selective dopamine D3receptor antagonist SB277011A. *Magn Reson Imaging*. 2007;25:811–20.
76. De Simoni S, Schwarz AJ, O'Daly OG, Marquand AF, Brittain C, Gonzales C, et al. Test-retest reliability of the BOLD pharmacological MRI response to ketamine in healthy volunteers. *Neuroimage*. 2013;64:75–90. <https://doi.org/10.1016/j.neuroimage.2012.09.037>
77. Deakin JFW, Lees J, McKie S, Hallak JEC, Williams SR, Dursun SM. Glutamate and the neural basis of the subjective effects of ketamine: a pharmaco-magnetic resonance imaging study. *Arch Gen Psychiatry*. 2008;65:154–64.
78. Anticevic A, Corlett PR, Cole MW, Savic A, Gancsos M, Tang Y, et al. N-methyl-D-aspartate receptor antagonist effects on prefrontal cortical connectivity better model early than chronic schizophrenia. *Biol Psychiatry*. 2015;77:569–80. <https://doi.org/10.1016/j.biopsych.2014.07.022>
79. Driesen NR, McCarthy G, Bhagwagar Z, Bloch M, Calhoun V, D'Souza DC, et al. Relationship of resting brain hyperconnectivity and schizophrenia-like symptoms produced by the NMDA receptor antagonist ketamine in humans. *Mol Psychiatry*. 2013;8:230–6.
80. Khalili-Mahani N, Niesters M, van Osch MJ, Oitzl M, Veer I, de Rooij M, et al. Ketamine interactions with biomarkers of stress: A randomized placebo-controlled repeated measures resting-state fMRI and PCASL pilot study in healthy men. *Neuroimage*. 2015;108:396–409. <https://doi.org/10.1016/j.neuroimage.2014.12.050>
81. Joles R, Doyle OM, Schwarz AJ, O'Daly OG, Brammer M, Williams SC, et al. Ketamine induces a robust whole-brain connectivity pattern that can be differentially modulated by drugs of different mechanism and clinical profile. *Psychopharmacology*. 2015;232:4205–18. <https://doi.org/10.1007/s00213-015-3951-9>
82. Páleníček T, Fújáčková M, Brunovský M, Balíková M, Horáček J, Gorman I, et al. Electroencephalographic spectral and coherence analysis of ketamine in rats: correlation with behavioral effects and pharmacokinetics. *Neuropsychobiology*. 2011;63:202–18. <https://doi.org/10.1159/000321803>
83. Ahnaou A, Huysmans H, Van De Castele T, Drinkenburg WHIM. Cortical high gamma network oscillations and connectivity: a translational index for anti-psychotics to normalize aberrant neurophysiological activity. *Transl Psychiatry*. 2017;7:1285 <https://doi.org/10.1038/s41398-017-0002-9>
84. Hudson MR, Sokolenko E, O'Brien TJ, Jones NC. NMDA receptors on parvalbumin-positive interneurons and pyramidal neurons both contribute to MK-801 induced gamma oscillatory disturbances: complex relationships with behaviour. *Neurobiol Dis*. 2020;134:104625 <https://doi.org/10.1016/j.nbd.2019.104625>
85. Moran RJ, Jones MW, Blockeel AJ, Adams RA, Stephan KE, Friston KJ. Losing control under ketamine: suppressed cortico-hippocampal drive following acute ketamine in rats. *Neuropsychopharmacology*. 2014;40:268–77. <https://doi.org/10.1038/npp.2014.184>
86. Vertes RP, Hoover WB. Projections of the paraventricular and paratenial nuclei of the dorsal midline thalamus in the rat. *J Comp Neurol*. 2008;508:212–37. <https://doi.org/10.1002/cne.21679>
87. Vertes RP. Differential projections of the infralimbic and prelimbic cortex in the rat. *Synapse*. 2004;51:32–58. <https://doi.org/10.1002/syn.10279>
88. Thompson KJ, Khajehali E, Bradley SJ, Navarrete JS, Huang XP, Slocum S, et al. DREADD agonist 21 is an effective agonist for muscarinic-based DREADDs in vitro and in vivo. *ACS Pharmacol Transl Sci*. 2018;1:61–72. <https://doi.org/10.1021/acspstci.8b00012>
89. Chan WY, McKinzie DL, Bose S, Mitchell SN, Witkin JM, Thompson RC, et al. Allosteric modulation of the muscarinic M4 receptor as an approach to treating schizophrenia. *Proc Natl Acad Sci USA*. 2008;105:10978–83. <https://doi.org/10.1073/pnas.0800567105>
90. Shah D, Blockx I, Guns P-J, De Deyn PP, Van Dam D, Jonckers E, et al. der Linden, Acute modulation of the cholinergic system in the mouse brain detected by pharmacological resting-state functional MRI. *Neuroimage*. 2015;109:151–9. <https://doi.org/10.1016/j.neuroimage.2015.01.009>
91. Byun NE, Grannan M, Bubser M, Barry RL, Thompson A, Rosanelli J, et al. Anti-psychotic drug-like effects of the selective M4 muscarinic acetylcholine receptor positive allosteric modulator VU0152100. *Neuropsychopharmacology*. 2014;39:1578–93. <https://doi.org/10.1038/npp.2014.2>
92. Kurimoto E, Nakashima M, Kimura H, Suzuki M. TAK-071, a muscarinic M1 receptor positive allosteric modulator, attenuates scopolamine-induced quantitative electroencephalogram power spectral changes in cynomolgus monkeys. *PLoS One*. 2019;14:e0207969 <https://doi.org/10.1371/journal.pone.0207969>

93. Vingerhoets C, Bakker G, Schranke A, van der Pluijm M, Bloemen OJN, Reneman L, et al. Influence of muscarinic M1 receptor antagonism on brain choline levels and functional connectivity in medication-free subjects with psychosis: a placebo controlled, cross-over study. *Psychiatry Res Neuroimaging*. 2019;290:5–13. <https://doi.org/10.1016/j.psychres.2019.06.005>
94. Power JD, Schlaggar BL, Petersen SE. Studying brain organization via spontaneous fMRI signal. *Neuron*. 2014;84:681–96. <https://doi.org/10.1016/j.neuron.2014.09.007>
95. C Canella, F Rocchi, S Noei, D Gutierrez-Barragan, L Coletta, A Galbusera, et al. Cortical silencing results in paradoxical fMRI overconnectivity, *BioRxiv*. 2020. <https://doi.org/10.1101/2020.08.05.237958>